

Anisotropic Transport Properties of CeRu₂Al₁₀

Hiroshi TANIDA*, Daiki TANAKA, Masafumi SERA, Chikako MORIYOSHI¹, Yoshihiro KUROIWA¹
Tomoaki TAKESAKA², Takashi NISHIOKA², Harukazu KATO², and Masahiro MATSUMURA²

Department of Quantum Matter, ADSM, Hiroshima University, Higashi-Hiroshima, Hiroshima 739-8530

¹*Department of Physics, Hiroshima University, Higashi-Hiroshima, Hiroshima 739-8530*

²*Graduate School of Integrated Arts and Science, Kochi University, Kochi 780-8520*

We studied the transport properties of CeRu₂Al₁₀ single crystals. All the transport properties show largely anisotropic behaviors below T_0 . Those along the a - and c -axes show similar behaviors, but are different from those along the b -axis. This suggests that the system could be viewed as a two-dimensional system. The results of the thermal conductivity and thermoelectric power could be explained by assuming the singlet ground state below T_0 . However, the ground state is not simple but has some kind of structure within a spin gap.

KEYWORDS: CeRu₂Al₁₀, spin gap, singlet ground state, Kondo semiconductor

The ternary rare-earth compound CeRu₂Al₁₀ has attracted much attention because of the mysterious transition at $T_0=27$ K.¹⁻³⁾ As for the long-range order (LRO) below T_0 , Strydom proposed magnetic ordering.¹⁾ However, Nishioka *et al.* pointed out that $T_0=27$ K is too high for RRu₂Al₁₀ with R=Ce because, even in GdRu₂Al₁₀, $T_N=16$ K; they insisted that the origin of the LRO below T_0 is nonmagnetic and proposed charge density wave (CDW) formation.²⁾ Matsumura *et al.* showed no evidence of magnetic ordering below T_0 from the results of ²⁷Al-NQR measurement and proposed the occurrence of structural phase transition below T_0 .³⁾ In our previous paper,⁴⁾ we studied the La substitution effect on CeRu₂Al₁₀ and the magnetic field effect on T_0 in order to clarify the nature of the LRO,⁴⁾ and found that T_0 is reduced by La substitution and disappears at $x \sim 0.45$ in Ce _{x} La_{1- x} Ru₂Al₁₀. The suppression of T_0 by a magnetic field along the easy magnetization axis was also observed. From these results, we concluded that the origin of the LRO below T_0 is magnetic. Considering the above points and a large magnetic entropy at T_0 , a decrease in the magnetic susceptibility below T_0 along all the crystal axes, the existence of a gap in many physical quantities, and a positive pressure effect on T_0 , we proposed that the LRO with a singlet ground state is formed below T_0 .⁴⁾ However, many physical properties remain to be explained from this standpoint, as mentioned in our previous paper.⁴⁾ In the present study, we measured the transport properties of CeRu₂Al₁₀ single crystal, focusing on their anisotropy to clarify the unusual nature in the LRO below T_0 .

Single crystals of Ce _{x} La_{1- x} Ru₂Al₁₀ ($x=1$ and 0.1) and CeFe₂Al₁₀ were prepared by the Al self-flux method. Hall resistivity was measured by the conventional four probe method below ~ 50 K. Thermal conductivity was measured by the conventional steady state method below ~ 50 K. Thermoelectric power was measured by the conventional differential method between 1.8 and 300 K.

Figure 1 shows the temperature (T) dependence of the Hall resistivity ρ_H of CeRu₂Al₁₀ measured at $H=5$ T,

which is applied along the a -, b -, and c -axes. ρ_H shows a roughly H linear dependence up to 5 T and the sign of ρ_H is positive in the entire temperature range studied here. ρ_H shows a large anisotropy depending on the applied magnetic field direction. ρ_H for $H \parallel b$ is the largest and that for $H \parallel a$ is the smallest. ρ_H for $H \parallel b$ increases with decreasing temperature in a paramagnetic region and increases largely after showing a kink at T_0 . ρ_H below T_0 shows no convex T dependence, which is expected when the gap is opened on the Fermi surface but shows a concave one. For $H \parallel c$, the T dependence of ρ_H in the entire temperature range is similar to that for $H \parallel b$, although its magnitude is much smaller than that for $H \parallel b$. The magnitude at the lowest temperature is about one third of that for $H \parallel b$. Noted that the anomaly at T_0 is much less pronounced than that for $H \parallel b$ and a small hump is seen at approximately $T \sim 17$ K. For $H \parallel a$, ρ_H is the smallest and the T dependence above ~ 20 K is very different from those for $H \parallel b$ and c . No anomaly is recognized at T_0 and a concave T dependence is seen down to ~ 17 K below ~ 25 K; in a paramagnetic region, its T dependence is very small and its magnitude is also much smaller than those for $H \parallel b$ and c . We emphasize that ρ_H below T_0 for $H \parallel b$ where the electrical current flows in the ac -plane shows very different behaviors from those for $H \parallel c$ and a . ρ_H for $H \parallel c$ is largest and that for $H \parallel a$ is smallest in the whole temperature range studied here. Although ρ_H for $H \parallel b$ and c show a kink at T_0 , that for $H \parallel a$ shows no anomaly. Although the T dependence is seen for $H \parallel b$ and c in a paramagnetic region, ρ_H for $H \parallel a$ is independent of temperature. If we estimate carrier concentration assuming a single carrier, we will obtain values of ~ 0.1 , ~ 0.02 , and ~ 0.06 /unit cell at $T=1.5$ K for $H \parallel a$, b , and c , respectively. At $T=35$ K, they are ~ 6.3 , ~ 1.2 , and ~ 2.0 /unit cell for $H \parallel a$, b , and c , respectively.

Figure 2 shows the T dependence of the thermal conductivity κ along the a -, b -, and c -axes. The T dependences and magnitudes of κ_a and κ_c are similar to each other but different from those of κ_b . κ_a and κ_c show a sharp dip at T_0 and a clear enhancement below T_0 . After showing a broad maximum at approximately $T \sim 24$ K, κ_a

*E-mail address: tany@hiroshima-u.ac.jp

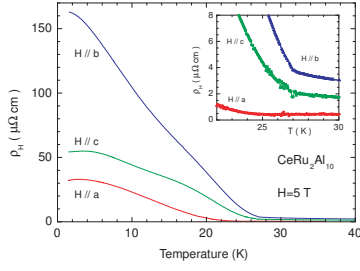


Fig. 1. (Color Online) Temperature dependence of Hall resistivity of $\text{CeRu}_2\text{Al}_{10}$ measured at $H=5$ T, where data were obtained by following the configurations of (i) $H \parallel a$, $I \parallel c$, $V_H \parallel b$, (ii) $H \parallel b$, $I \parallel a$, $V_H \parallel c$, and (iii) $H \parallel c$, $I \parallel a$, $V_H \parallel b$, respectively. Here, V_H is the Hall voltage.

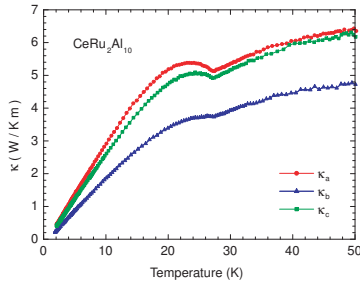


Fig. 2. (Color Online) Temperature dependence of thermal conductivity of $\text{CeRu}_2\text{Al}_{10}$ along the a -, b -, and c -axes.

and κ_c decrease with decreasing temperature. Although κ_b also shows a dip at T_0 , it is much less pronounced than in κ_a and κ_c and no enhancement below T_0 is seen. κ along the three crystal axes is roughly proportional to the temperature below ~ 12 K down to 2 K. A negative intercept is obtained if it is extrapolated down to $T=0$. At low temperatures below 2 K, κ is expected to show a T^3 dependence, which originates from the specific heat of phonon because the sound velocity and phonon mean free path are expected to be independent of temperature at low temperatures. Since the magnitude of the electrical resistivity ρ is large, the electronic contribution to κ is small. Even in the case with the smallest ρ along the a -axis, the electronic contribution is estimated to be $\sim 2\%$ at $T=20$ K assuming the Wiedemann-Franz law. Thus, thermal current is mainly carried by phonon. Then, the observed anisotropy of κ is considered to be dominated by the anisotropy of the phonon contribution.

Figure 3 shows the T dependence of the thermoelectric power S of $\text{Ce}_{0.1}\text{La}_{0.9}\text{Ru}_2\text{Al}_{10}$ along the a -, b -, and c -axes. S is negative at high temperatures and is positive at low temperatures. All the results show similar T dependences and their magnitudes are also close to each other. At high temperatures, S shows a roughly T -linear dependence with a negative slope. At $T \sim 10$ K, a distinct positive peak is observed. Considering the results of ρ and specific heat of this sample, this positive peak is expected to originate from the Kondo effect. A very broad hump at ~ 150 K may result from the crystalline-electric-field (CEF) effect.^{5,6)}

Figure 4 shows the T dependence of S of $\text{CeRu}_2\text{Al}_{10}$

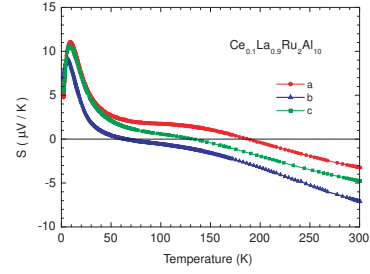


Fig. 3. (Color Online) Temperature dependence of thermoelectric power of $\text{Ce}_{0.1}\text{La}_{0.9}\text{Ru}_2\text{Al}_{10}$ along the a -, b -, and c -axes.

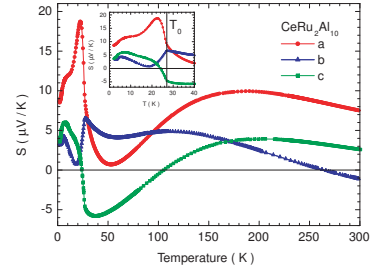


Fig. 4. (Color Online) Temperature dependence of thermoelectric power of $\text{CeRu}_2\text{Al}_{10}$ along the a -, b -, and c -axes.

along the a -, b -, and c -axes. All the results show a broad maximum at $T \sim 150$ K, which is much more pronounced than those of $\text{Ce}_{0.1}\text{La}_{0.9}\text{Ru}_2\text{Al}_{10}$. This maximum may reflect the CEF splitting, which is expected to be larger than ~ 300 K. Although a change of sign is observed in S_c between ~ 25 K and ~ 100 K, and the magnitude of maximum differs between S_a , S_c , and S_b , the overall T dependences are similar to each other along three crystal axes in a paramagnetic region. Namely, a broad maximum at high temperatures of approximately ~ 150 K, a decrease down to ~ 50 K, and an increase down to T_0 . The increase in S below 50 K down to T_0 seems to be associated with the large increase in ρ in the same temperature region. S below T_0 shows a very anisotropic and anomalous T dependence as is shown in the inset of Fig. 4. The most characteristic feature is that although S_a and S_c show a steep increase below T_0 , S_b shows a steep decrease below T_0 . This again suggests that the nature in the ac -plane is different from that along the b -axis. Below T_0 , S_a shows a pronounced maximum at $T \sim 22$ K and decreases with decreasing temperature. A pronounced shoulder is seen at $T \sim 8$ K. S_c also shows a steep increase below T_0 . After showing a very small concave curvature at ~ 14 K, it shows a maximum at $T \sim 6$ K. On the other hand, S_b shows a steep decrease below T_0 and after exhibiting a broad minimum at $T \sim 18$ K, it shows a maximum at $T \sim 6$ K. Thus, S shows two characteristic behaviors. One is a steep increase in S_a and S_c and a steep decrease in S_b below T_0 . Another is the existence of a broad maximum at $6 \sim 8$ K along all the crystal axes.

The present results of ρ_H , κ , and S strongly suggest that the origin of the mysterious LRO below T_0 exists in the ac -plane. First, we consider the nature of LRO

below T_0 from the standpoint of the crystal structures. The powder X-ray diffraction was examined by BL02B2 in SPring-8. The lattice constants of $\text{CeRu}_2\text{Al}_{10}$ are $a=9.12233(4)$, $b=10.27486(4)$, and $c=9.18353(4)\text{\AA}$ and those of $\text{CeFe}_2\text{Al}_{10}$ are $a=9.00628(6)$, $b=10.23105(7)$, and $c=9.07838(6)\text{\AA}$ at room temperature. These values are obtained by Rietveld analysis. Although the valence of the Ce ion in $\text{CeRu}_2\text{Al}_{10}$ is considered to be +3, the Ce ion in $\text{CeFe}_2\text{Al}_{10}$ is considered to be situated in a valence fluctuation regime from the magnetic susceptibility.^{2,7)} In our previous study,²⁾ we showed that the ρ of $\text{CeRu}_2\text{Al}_{10}$ becomes closer to that of $\text{CeFe}_2\text{Al}_{10}$ with increasing pressure. This suggests that some hint on the LRO in $\text{CeRu}_2\text{Al}_{10}$ could be obtained from the difference of the lattice constants between these two compounds. Here, we consider the ratio (Ru/Fe) of each lattice constant of $\text{CeRu}_2\text{Al}_{10}$ to that of $\text{CeFe}_2\text{Al}_{10}$. The ratios are 1.01289, 1.00428, and 1.01147 for the a -, b -, and c -axes, respectively. The magnitude of shrinkage in the ac -plane is more than twice as large as that along the b -axis. In the ac -plane, the magnitude of shrinkage for the a -axis is nearly the same as that for the c -axis. Considering these results, we conjecture that the LRO below T_0 mainly originates from the ac -plane.

Here, we describe the characteristics of the crystal structure in detail. Figures 5(a) and 5(b) show the crystal structures of $\text{CeRu}_2\text{Al}_{10}$, which are viewed from the c - and a -axes, respectively. In these figures, Ru-Al 1~Al 5 are connected by lines. By considering the present results showing that the transport properties in the ac -plane are different from those along the b -axis, the above-mentioned anisotropy of lattice constants and the fact that the Al 5 site is a specific site from the NQR measurement, we consider that a layer formed by Ce, Ru, and Al 1~Al 4 is separated by Al 5 ions along the b -axis. Although Al 5 ions lie on a straight line along the b -axis, as shown in Fig. 5(b), when viewed from the a -axis, the ions form a zigzag structure along the b -axis when viewed from the c -axis, as shown in Fig. 5(a). In the upper and lower planes of this layer, there exist Ce and Al 1~Al 4 ions. Ru ions are situated in a middle of this layer along the b -axis. Although Ce ions in the upper and lower planes are equivalent, here, we distinguish them using different colors (black and gray) to see the physical meaning easily in the present discussion. It should be noted that Ce and Al 1~Al 4 ions do not lie on the same plane. Figure 5(c) shows the crystal structure viewed from the b -axis. The Ce ions on the upper plane are surrounded by a large square formed by Al 2 and Al 3 ions. A small square formed by Al 1 and Al 4 ions which are situated just above Ce ion in a lower plane, is situated just in the middle of four large squares. Large and small squares are connected by two kinds of rhombuses formed by Al 1-Al 3 and Al 2-Al 4 ions. Here, the two kind of squares are slightly distorted and the two kinds of rhombuses are not equivalent, which leads to a small difference between the lattice constants a and c . Figure 5(d) shows a schematic picture of the crystal viewed from the $[10\bar{1}]$ direction. In this figure, it is seen that a layer formed by Ce, Ru, and Al 1~Al 5 ions is constructed by a trapezoid with the staggered arrangement along the $[101]$

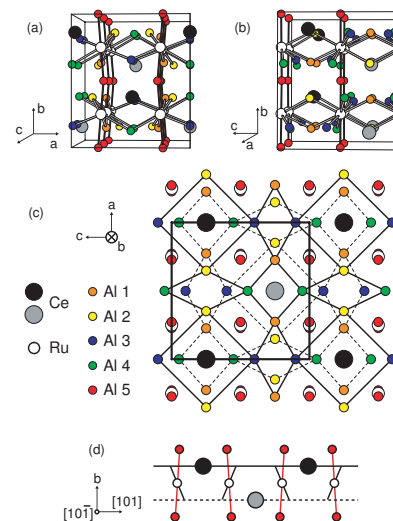


Fig. 5. (Color Online) Crystal structure of $\text{CeRu}_2\text{Al}_{10}$ viewed from (a) c -axis, (b) a -axis, (c) b -axis, and (d) $[10\bar{1}]$ direction. Although all the Ce ions are equivalent, here, we distinguish Ce ions in the upper plane (black circle) from those in the lower plane (gray circle) of the layer formed by Ce, Ru, and Al 1~Al 4. The upper and lower planes are drawn by a solid and dotted lines, respectively.

direction. Ce ions are situated in the middle of the base of a trapezoid. Thus, the crystal structure of $\text{CeRu}_2\text{Al}_{10}$ could be viewed as a two-dimensional system.

Now, we discuss the present results. First, we discuss thermal conductivity. As mentioned above, the contribution of the charge carrier can be neglected and thermal current is mainly carried by phonons. Then, κ is expressed as $C_{ph}v_sl_{ph}/3$. Here, C_{ph} , v_s , and l_{ph} are the specific heat of phonon, sound velocity, and mean free path of phonon, respectively. Since C_{ph} does not depend on the crystal axis, the anisotropy of κ originates from that of v_s or l_{ph} . At high temperatures, κ_b is the smallest. This could be explained by considering the existence of the zigzag alignment of the Al 5 site along the b -axis, which is shown in Fig. 5(a). At around T_0 , although a clear dip at T_0 and a clear enhancement below T_0 are observed in κ_a and κ_c , the anomalies at T_0 in κ_b are much less pronounced. These suggest that the origin of the LRO lies in the ac -plane, and a small anomaly along the b -axis seems to appear as a secondary effect. In our previous paper,⁴⁾ we proposed that the enhancement of κ below T_0 could be explained as follows. The absolute value of ρ is large and so κ is dominated by phonons. Below T_0 , by forming a singlet pair between Ce ions, the vibration of Ce ions is expected to be suppressed more than when each Ce ion vibrates independently above T_0 . As a result, the mean free path of phonons could be enhanced below T_0 . This causes the enhancement of κ below T_0 . At present, we do not know how v_s behaves around T_0 . The above should be confirmed in the future studies.

Next, we discuss the Hall effect. Before discussing the Hall effect, we mention the results of ρ . ρ shows a steep increase below T_0 along all the crystal axes.²⁾ This simply suggests that the gap is opened on the Fermi surface

rather isotropically. However, such a situation could occur only when the almost complete nesting of the Fermi surface takes place. However, this is quite difficult to expect in the present three-dimensional complex sample. Furthermore, if such a complete isotropic nesting takes place below T_0 , ρ_H should increase below T_0 in all the applied field directions. However, no such behavior is observed. No anomaly is seen in ρ_H for $H \parallel a$ at T_0 . This denies the gap opening at least for $H \parallel a$ and suggests that it is better to find other origins of the anomalous transport properties below T_0 , except the gap opening on the Fermi surface. ρ_H shows the clearest anomaly at T_0 for $H \parallel b$ and the largest magnitude. Here, current flows in the ac -plane. This suggests that the transport property in the ac -plane is most largely affected by the LRO at T_0 . In a paramagnetic region, although ρ_H shows an increase with decreasing temperature down to T_0 for $H \parallel a$ and c , that for $H \parallel b$ is temperature-independent in the temperature range studied here. The former could be ascribed to a decrease in carrier concentration with decreasing temperature, which seems to be consistent with the T dependence of ρ , or to the anomalous Hall effect. However, no T dependence of ρ_H for $H \parallel a$ where current flows in the bc -plane is observed, and its magnitude is much smaller than those for $H \parallel b$ and c above T_0 . Thus, both below and above T_0 , it is difficult to estimate the real carrier concentration in $\text{CeRu}_2\text{Al}_{10}$. Further studies are necessary to clarify the origin of the anisotropic behavior of ρ_H .

Next, we discuss thermoelectric power, which shows the most anisotropic behavior below T_0 among the three transport properties studied here. S is expressed as

$$S = \frac{1}{eT} \frac{\int \sigma(\varepsilon)(\varepsilon - \zeta) \frac{\partial f(\varepsilon)}{\partial \varepsilon} d\varepsilon}{\int \sigma(\varepsilon) \frac{\partial f(\varepsilon)}{\partial \varepsilon} d\varepsilon}, \quad (1)$$

where, $f(\varepsilon)$ is the Fermi distribution function and ζ is the Fermi energy. S is expressed by Mott formulation as

$$S = \frac{\pi^2 k_B^2 T}{3e} \left[\frac{1}{N(\varepsilon)v^2} \frac{\partial N(\varepsilon)v^2}{\partial \varepsilon} + \frac{1}{\tau(\varepsilon)} \frac{\partial \tau(\varepsilon)}{\partial \varepsilon} \right]_{\varepsilon=\zeta}, \quad (2)$$

where $N(\varepsilon)$, v , and $\tau(\varepsilon)$ are the density of states, Fermi velocity, and relaxation time of conduction electrons, respectively. In order to obtain a large magnitude of S , a large energy dependence of $\tau(\varepsilon)$ at around $\varepsilon = \zeta$ as a function of energy is necessary. ρ is determined by the magnitude of $\tau(\varepsilon)$ at $\varepsilon = \zeta$ itself. In S , its magnitude is important but the energy dependence of $\tau(\varepsilon)$, $\partial \tau(\varepsilon)/\partial \varepsilon$ is more important. Namely, the inelastic scattering of charge carriers associated with the term $(\varepsilon - \zeta)$ in eq. (1) is essentially important to understand the anomalous behavior in S . When the gap is opened on the Fermi surface, the first term in eq. (2) originating from $N(\varepsilon)$, which is affected by the gap opening, is also important. However, as mentioned above, it is expected that the gap is not opened at least isotropically on the Fermi surface. Thus, we ascribe the anomalous T dependence of S below T_0 to the energy dependence of $\tau(\varepsilon)$ at around $\varepsilon = \zeta$. It is known that the Kondo impurity induces a

large anomalous T dependence in S at low temperatures. Kondo explained this unusual behavior of S by considering the fourth-order perturbation J^3V .⁸⁾ The potential scattering term V is introduced for $\tau(\varepsilon)$ to be an odd function of energy. Peshchel and Fulde calculated S for a compound with a singlet ground state by considering the third-order perturbation J^2V .⁵⁾ The existence of CEF splitting with a singlet ground state reduces the perturbation from the fourth order to the third order. They showed that S exhibits a Schottky-type anomaly in its T dependence. This originates from the inelastic scattering of charge carriers by a spin-flip scattering between the CEF ground state and the excited state. Namely, in such a CEF level scheme, the higher the energy, the larger the spin-flip scattering probability because the magnetic excited state is situated on the higher energy side. In our previous paper,⁴⁾ we proposed that the singlet ground state is formed below T_0 . The present anomalous T dependence of S below T_0 could be explained using the above mechanism proposed by Peshchel and Fulde. In the model by Peshchel and Fulde, the energy splitting between two levels is temperature-independent and so a Schottky-type anomaly is obtained. However, in the present case, the singlet-triplet splitting is induced below T_0 , which leads to a discontinuous enhancement below T_0 . The difference in the sign of dS/dT between the ac -plane and the b -axis just below T_0 could be ascribed to a difference in the sign of V , although its microscopic mechanism is as yet unknown. A maximum of S together with a shoulder of ρ at $T \sim 8$ K suggests a change in the energy dependence of $\tau(\varepsilon)$ at around this temperature. This suggests the existence of some kind of structure within a spin gap.

To conclude, we studied the thermal transport properties in $\text{CeRu}_2\text{Al}_{10}$ single crystal. All the transport properties show very anisotropic behaviors below T_0 . Those in the ac -plane are very different from those along the b -axis, which suggests that the system could be viewed as a two-dimensional system. The results of ρ_H deny a gap opening on the Fermi surface at least for $H \parallel a$ and suggest the existence of other mechanisms of the anomalous transport properties except the gap opening on the Fermi surface. The results of κ and S below T_0 could be explained by assuming the LRO with a singlet ground state. However, the ground state is not simple but has a structure within a spin gap.

- 1) A. M. Strydom; *Physica B* **404** (2009) 2981.
- 2) T. Nishioka, Y. Kawamura, T. Takesaka, R. Kobayashi, H. Kato, M. Matsumura, K. Kodama, K. Matsubayashi, and Y. Uwatoko; *J. Phys. Soc. Jpn.* **78** (2009) 123705.
- 3) M. Matsumura, Y. Kawamura, S. Edamoto, T. Takesaka, H. Kato, T. Nishioka, Y. Tokunaga, S. Kambe, and H. Yasuoka; *J. Phys. Soc. Jpn.* **78** (2009) 123713.
- 4) H. Tanida, D. Tanaka, M. Sera, C. Moriyoshi, Y. Kuroiwa, T. Takesaka, T. Nishioka, H. Kato, and M. Matsumura; *J. Phys. Soc. Jpn.* **79** (2010) 043708.
- 5) I. Peshchel and P. Fulde; *Z. Physik* **238** (1970) 99.
- 6) S. Maekawa, S. Kashiba, M. Tachiki, and S. Takahashi; *J. Phys. Soc. Jpn.* **55** (1986) 3194.
- 7) Y. Muro, K. Motoya, Y. Saiga, and T. Takabatake; *J. Phys. Soc. Jpn.* **78** (2009) 083707.
- 8) J. Kondo; *Prog. Theor. Phys.* **34** (1965) 372.